

can serve as models for future studies on the fitness effects of mitochondrial mutations and as models for investigating mitochondrial genetic disorders. Furthermore, the high rate and strongly biased pattern of mtDNA mutation detected here increase the probability of parallel mutations. The high potential for homoplasmy must be considered when using mtDNA for evolutionary studies and when investigating the occurrence of recombination in mitochondrial genomes (29, 30).

References and Notes

1. L. Vigilant, M. Stoneking, H. Harpending, K. Hawkes, A. C. Wilson, *Science* **253**, 1503 (1991).
2. S. Horai, K. Hayasaka, R. Kondo, K. Tsugane, N. Takahata, *Proc. Natl. Acad. Sci. U.S.A.* **92**, 532 (1995).
3. T. J. Parsons et al., *Nature Genet.* **15**, 363 (1997).
4. N. Howell, I. Kubacka, D. A. Mackey, *Am. J. Hum. Genet.* **59**, 501 (1996).
5. E. Jazin et al., *Nature Genet.* **18**, 109 (1998).
6. S. Pääbo, *Am. J. Hum. Genet.* **59**, 493 (1996).
7. J. W. Drake, B. Charlesworth, D. Charlesworth, J. F. Crow, *Genetics* **148**, 1667 (1998).
8. M. Lynch et al., *Evolution* **53**, 645 (1999).
9. R. Okimoto, J. L. Macfarlane, D. O. Clary, D. R. Wolstenholme, *Genetics* **130**, 471 (1992).
10. Amplifications of mtDNA were performed in 50- μ l reactions containing 67 mM tris-HCl (pH 8.8), 6.7 mM MgCl₂, 16.6 mM (NH₄)₂SO₄, 10 mM β -mercaptoethanol, 1 mM each of dGTP, dATP, dTTP, and dCTP, 0.5 μ M of each primer, 10 to 100 ng of genomic DNA, and 2.5 U of *Thermus aquaticus* DNA polymerase (Perkin Elmer). Amplification was carried out by 35 cycles of denaturation at 94°C for 1 min, annealing at 52° to 55°C for 1 min, and extension at 72°C for 2 min. Primer sequences, positions spanned, and PCR product sizes are listed in Web table 1 (26). Primers were designed to the published sequence of N2 *C. elegans* mtDNA (72). PCR products were separated in a 2% SeaPlaque GTG (FMC Bioproducts) agarose gel. Bands were excised and purified with a QIAquick gel extraction kit (Qiagen). The purified PCR product was used as a template for cycle sequencing with dRhodamine dye terminators. PCR primers were used for sequencing reactions along with internal primers where necessary. Cycle sequencing was carried out by 25 cycles of denaturation at 96°C for 30 s, annealing at 50°C for 15 s, and extension at 60°C for 4 min. Unincorporated dye terminators were removed with Micro Bio-Spin Chromatography Columns (Bio-Rad). Sequences were determined with an ABI Prism 377 automated DNA sequencer (Perkin-Elmer). Sequences were aligned to the published N2 mtDNA sequence (9) with the ESEE computer alignment program [E. Cabot, Eyeball Sequence Editor (ESEE), Version 3.01 (1997)]. Two mutations were detected in the N2 progenitor of the MA lines, relative to the published sequence (5011 G→A, 8429 A→G). The first mutation is at a nonsynonymous site, replacing alanine with valine. The second is at a synonymous site. All substitution and indel mutations were confirmed by sequences from both strands of DNA.
11. L. L. Vassilieva and M. Lynch, *Genetics* **151**, 119 (1999).
12. L. Vassilieva, A. M. Hook, M. Lynch, *Evolution* **54**, 1234 (2000).
13. If we use a mutation rate per base per generation (μ) for all mutations excluding those associated with repetitive sequence, $\mu = 1.1 \times 10^{-7}$. With 214 generations and 10,428 positions, the mean number of mutations per line is 0.2455. Assuming a Poisson distribution, the expected number of lines with 0, 1, or 2 mutations is 57, 16, and 1, respectively. Alternatively, if we use the proportion of lines with 0 mutations to calculate the total mutation rate, $\mu = 3.5 \times 10^{-7}$ per site per generation and the expected number of lines with 1 or 2 mutations is 14.8 and 1.9, respectively.
14. T. Lindahl, *Nature* **362**, 709 (1993).
15. X. Xia, M. S. Hafner, P. D. Sudman, *J. Mol. Evol.* **43**, 32 (1996).
16. Natural geographic isolates of *C. elegans* were obtained from the *Caenorhabditis* Genetics Center (CGC) at the University of Minnesota. Initial isolation and characterization of natural isolates is described by J. Hodgkin and T. Doniach [*Genetics*, **146**, 149 (1997)] and can be obtained on the CGC server (<http://biosci.umn.edu/CGC/Strains/strains.htm>). The same sequences (10,428 bp) are analyzed. Between N2 and RC301 the following substitutions were observed: 19 T→C, 8 A→G, 1 T→G, and 1 T→A.
17. No significant difference in transition bias is detected between the natural isolates and the MA lines ($P > 0.05$).
18. S. Yokobori et al., *Genetics* **153**, 1851 (1999).
19. S. Asakawa et al., *J. Mol. Evol.* **32**, 511 (1991).
20. G. Preparata and C. Saccone, *J. Mol. Evol.* **26**, 7 (1987).
21. W. K. Thomas and A. C. Wilson, *Genetics* **128**, 269 (1991).
22. Twenty-nine total substitutions are observed between N2 and RC301, and 26 of these are synonymous. On the basis of the proportion of replacements in MA lines (8/14), we would expect 34.7 replacement changes between N2 and RC301 in the absence of selective constraints. Consequently, the efficiency of selection on replacement mutations can be expressed as $1 - (3/34.7) = 0.914$, giving a width of the selective sieve equal to 0.086.
23. We have sequenced 8554 bp of mtDNA from the PB800 strain of *C. briggsae* as in (10). The PB800 strain is available from the CGC.
24. W. Habano, S. Nakamura, T. Sugai, *Oncogene* **17**, 1931 (1998).
25. We have analyzed the same sequences (10,428bp) from 31 natural isolates of *C. elegans*. No obvious disruptions in coding function are observed.
26. Supplementary data are available at Science Online at www.sciencemag.org/feature/data/1050947.shl.
27. For GeneScan analysis the region was amplified with the primer ND1-B(F) and the fluorescently labeled primer ND1-D(R)-HEX. Amplifications were performed as in (10). Samples were separated on an ABI 377 Automated Sequencer (Perkin-Elmer) with TAMRA 500 internal size standards.
28. D. C. Wallace, *Science* **283**, 1482 (1999). An updated list of known mtDNA mutations involved in human diseases is listed in *Neuromusc. Disord.* **9**, 9 (1999).
29. A. Eyre-Walker, N. H. Smith, J. Maynard Smith, *Proc. R. Soc. London Ser. B* **266**, 477 (1998).
30. P. Awadalla, A. Eyre-Walker, J. Maynard Smith, *Science* **286**, 2524 (1999).
31. Supported by a University of Missouri Research Board grant (to W.K.T.) and NIH grant R01-GM36827 (to M.L.).

31 March 2000; accepted 10 August 2000

Resetting of Circadian Time in Peripheral Tissues by Glucocorticoid Signaling

Aurélio Balsalobre,¹ Steven A. Brown,¹ Lysiane Marcacci,¹ François Tronche,² Christoph Kellendonk,^{2*} Holger M. Reichardt,² Günther Schütz,² Ueli Schibler^{1†}

In mammals, circadian oscillators reside not only in the suprachiasmatic nucleus of the brain, which harbors the central pacemaker, but also in most peripheral tissues. Here, we show that the glucocorticoid hormone analog dexamethasone induces circadian gene expression in cultured rat-1 fibroblasts and transiently changes the phase of circadian gene expression in liver, kidney, and heart. However, dexamethasone does not affect cyclic gene expression in neurons of the suprachiasmatic nucleus. This enabled us to establish an apparent phase-shift response curve specifically for peripheral clocks in intact animals. In contrast to the central clock, circadian oscillators in peripheral tissues appear to remain responsive to phase resetting throughout the day.

Daily rhythms in gene expression, physiology, and behavior persist under constant conditions and must, therefore, be driven by self-sustained biological oscillators called circadian clocks [for reviews, see (1, 2)]. Circadian clocks can count time only approximately and must be adjusted every day by the photoperiod in order to be in harmony with the outside world. In

mammals, light signals perceived by the retina are transmitted directly to the suprachiasmatic nucleus (SCN) via the retino-hypothalamic tract (3). The SCN, located in the ventral part of the hypothalamus, is thought to contain the master pacemaker, which synchronizes all overt rhythms in physiology and behavior (4).

In most systems, circadian oscillations rely on a negative feedback loop in gene expression that involves multiple clock genes. In *Drosophila*, the repertoire of essential clock genes includes *period* (*per*), *timeless* (*tim*), *clock* (*clk*), *cycle* (*cyc*), *doubletime* (*dbt*), *cryptochrome* (*cry*), and *vri* (*vrl*) (1, 5). During the past few years, one or more mammalian homologs to all of these genes have been uncovered. These include *Per1*, *Per2*, and *Per3*, *Tim*, *Clock*, *Bmal1*, *Tau*, *Cry1* and *Cry2*, and *E4bp4* (1, 5, 6).

Molecular oscillators may exist in most pe-

¹Département de Biologie Moléculaire, Sciences II, Université de Genève, 30 Quai Ernest Ansermet, CH-1211 Genève, Switzerland. ²Molecular Biology of the Cell, Deutsches Krebsforschungszentrum, Im Neuenheimer Feld 280, 69120 Heidelberg, Federal Republic of Germany.

*Present address: Center for Neurobiology and Behavior, 722 West 168th Street, Research Annex, New York, NY 10032, USA

†To whom correspondence should be addressed. E-mail: ueli.schibler@molbio.unige.ch

REPORTS

ripheral cells of *Drosophila* (7), zebrafish (8), and mammals (9, 10). In *Drosophila* and zebrafish, the peripheral clocks can be entrained directly by light (11–14). In mammals, it is thought that the phase of these peripheral timekeepers is reset by signals regulated by the SCN pacemaker (10). Because serum induces circadian gene expression in cultured rat-1 fibroblasts (9), one or more blood-borne factors must stimulate signal transduction pathways that influence the molecular oscillators in peripheral cells. Glucocorticoid hormones are particularly attractive candidates, because (i) they are secreted in daily cycles (15) and (ii) the glucocorticoid receptor (GR) is expressed in most peripheral cell types, but not in SCN neurons (16, 17). The second point would be consistent with glucocorticoids as entraining signals, given that circadian gene expression has a different phase angle in the SCN and in peripheral tissues (18).

We first investigated whether a 1-hour treatment with the glucocorticoid dexamethasone (19) can induce circadian gene expression in rat-1 fibroblasts (Fig. 1). This treatment rapidly activates *Per1* expression (Fig. 1A) but, in contrast to a serum shock (9), does not activate *Per2* mRNA levels above the slightly induced levels seen after treatment with the solvent alone (ethanol at 0.001%). We followed the accumulation pattern of circadian mRNAs during the 44 hours after the dexamethasone treatment (Fig. 1B). Similar to serum and unlike the solvent alone (Fig. 1C), dexamethasone elicits robust circadian gene expression of the clock genes *Per1*, *Per2*, *Per3*, and *Cry1* and the clock-controlled genes *Rev-erba* and *Dbp*.

Next, we wished to determine whether dexamethasone can also affect peripheral oscillators in vivo. To discriminate between direct actions of this glucocorticoid analog on peripheral cell types and indirect actions via the SCN, we examined whether the absence of GR expression in the SCN of rats (16, 17) also applies to mice. To this end, we hybridized mouse coronal brain sections (20) to a GR antisense RNA probe (21). Although strong to moderate signals

for GR mRNA can be observed for most brain regions (Fig. 2), few if any silver grains could be detected over the two SCNs (Fig. 2B) irrespective of the time of day at which the mice were killed (22). This suggests that GR mRNA does not accumulate to physiologically important levels in mouse SCN neurons. Hence, the effects of dexamethasone on circadian gene expression in peripheral tissues are unlikely to be mediated via the central SCN pacemaker. This hypothesis is confirmed by the inability of dexamethasone to shift the phase of the SCN (23).

Next, we measured the effect of dexamethasone on circadian liver gene expression in vivo. Dexamethasone 21-phosphate transiently induces *Per1* expression at all examined time points (24). If mice were injected before or during zenith levels (ZTs) at which *Per1* mRNA accumulation normally reaches such levels (ZT6 to ZT14), injection resulted in prolonged and/or stronger expression of *Per1* (e.g., injections at ZT21 or ZT8). However, if the injections were performed after *Per1* mRNA peak expression, a new surge of *Per1* expression was induced (see injection at ZT14 in Fig. 3A). Dexamethasone injection also resulted in transient phase shifts. For example, when dexamethasone was injected at ZT14, *Per1* expression was considerably delayed on the following day (Fig. 3A), although, in these experiments, circadian *Per1* gene expression was somewhat confounded by the dexamethasone-induced transient burst of *Per1* expression. To determine dexamethasone-induced phase shifts more accurately, we recorded the high-amplitude expression cycles of *Dbp* and *Rev-erba*, two genes that are not induced transiently by dexamethasone.

To examine the response of peripheral oscillators around the clock, we injected mice with dexamethasone at 10 time points, and we monitored the temporal *Dbp* and *Rev-erba* mRNA accumulation profiles for 36 to 60 hours. The data obtained for four different times of dexamethasone injection (ZT1, ZT5, ZT14, and ZT21) are compared with the data obtained with a control injection of solvent at ZT21 (Fig. 3, B and C). The control injections did not

affect circadian gene expression at ZT1, ZT3, ZT5, ZT8, and ZT21 (22). On the basis of these data, we estimated that strong phase delays were observed when dexamethasone was injected at ZT14 and ZT21, whereas injection of dexamethasone at ZT1 resulted in a phase advance (Fig. 3, B and C). In contrast, injection at ZT5 caused little if any change in the phase angle of *Dbp* and *Rev-erba* mRNA expression (Fig. 3, B and C). An apparent phase-shift response curve (aPRC) (25) for liver was ob-

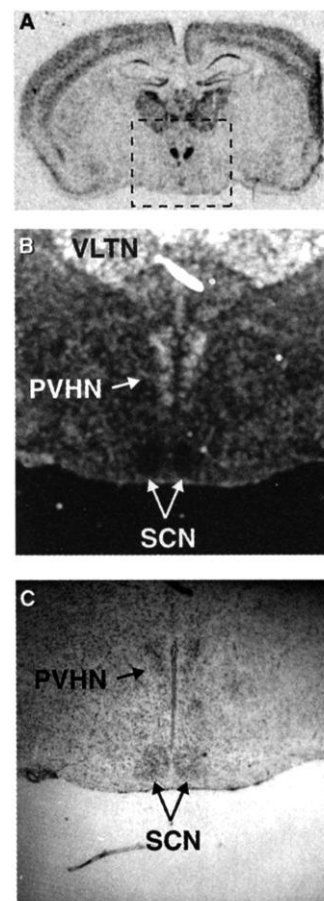
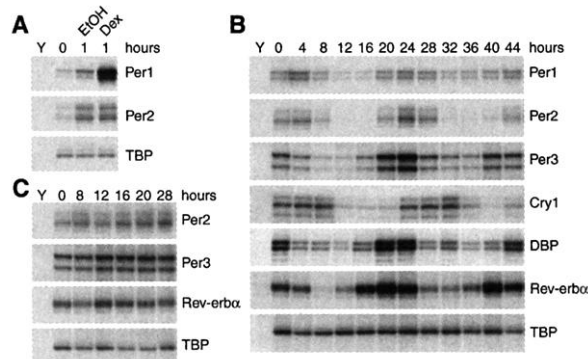


Fig. 2. GR mRNA does not accumulate to detectable levels in the SCN. Coronal brain sections containing the SCN were hybridized in situ to a 0.5 Kb ³⁵S-labeled GR antisense RNA probe spanning exons 6 through 9. After hybridization, sections were exposed to film for 1 week (A) and then were coated with Kodak NTB2 autoradiographic emulsion (KODAK GmbH, Stuttgart, Germany) and exposed for 1 month at 4°C (B). After development of the emulsion, sections were colored with cresyl violet to stain nuclei (C). (A) Autoradiography of a coronal section harvested at ZT6. (B) Dark-field photograph of the in situ hybridized hypothalamus region (hybridization signals appear as reduced silver grains in white). VLTN, ventrolateral thalamic nucleus; PVHN, Paraventricular hypothalamic nucleus. (C) Light-field photograph of the section presented in (B), showing cresyl violet-stained cell nuclei. Similar results were obtained at all other times examined (ZT2, ZT10, ZT14, ZT18, and ZT22) (22). Magnification of (B) and (C) is threefold that of (A).

Fig. 1. Dexamethasone induces circadian gene expression in rat-1 fibroblasts grown in tissue culture. At the indicated time, whole cell RNA was extracted and examined by ribonuclease protection. The antisense RNA probes are indicated at the right hand side of the panels. TBP mRNA (a transcript that is not induced by dexamethasone) served as an internal control. Y (yeast RNA only) served as a negative control. (A) Induction of *Per1* expression by dexamethasone (Dex). EtOH, solvent treatment. (B) Induction of circadian gene expression by dexamethasone. (C) Injection of the solvent alone does not induce circadian gene expression in vitro.



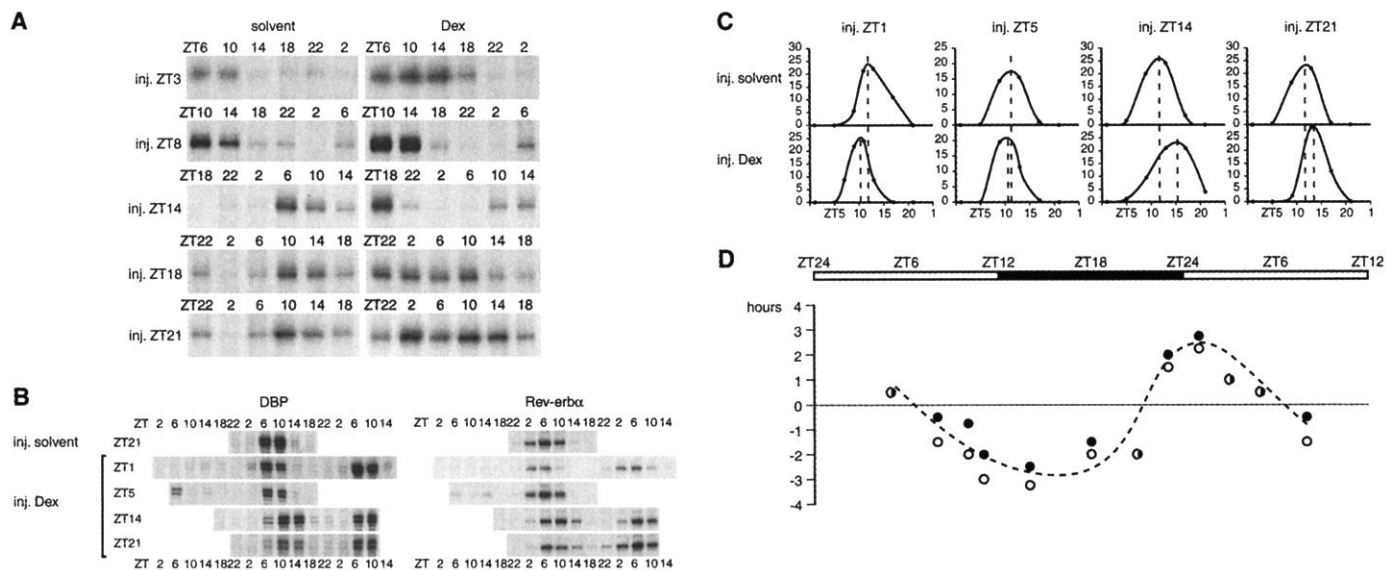
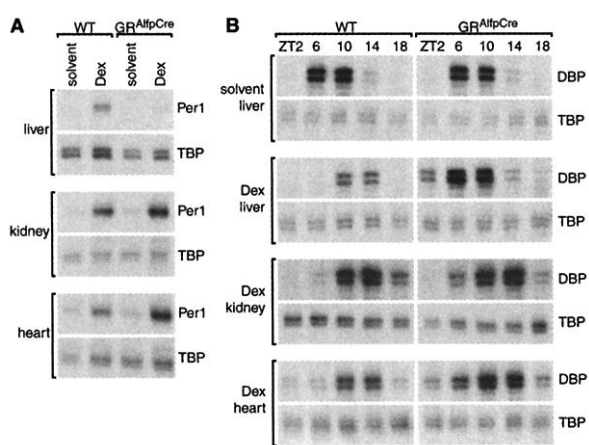


Fig. 3. Dexamethasone induces phase shifts in circadian gene expression in the periphery but not in the SCN. Dexamethasone-phosphate (Dex, 400 $\mu\text{g}/\text{ml}$ in PBS) or solvent (PBS with 1.5 $\mu\text{l}/\text{ml}$ of ethanol) were injected at different times into mice (2 $\mu\text{g}/\text{g}$ body weight). Animals were killed after the times indicated. In each experiment, a TBP antisense RNA probe was included as an internal control (22) for a transcript whose cellular concentration remains constant throughout the day. (A) Circadian *Per1* expression in liver after dexamethasone injection. Compared with the stimulation of *Per1* expression observed *in vitro*, the activation observed *in vivo* was delayed by 2 to 4 hours (Fig. 1A) (22). (B) The levels

of DBP and *Rev-erb α* mRNAs were determined by ribonuclease protection experiments. (C) The signals obtained in ribonuclease protection assays for DBP and TBP transcripts were determined by scanning the gels. The relative levels of DBP transcripts are given as DBP/TBP mRNA signal ratios on the y axis. Dotted lines indicate peak expression; differences indicate phase shift. (D) Dexamethasone-induced phase-shifts in the expression of DBP and *Rev-erb α* transcripts were recorded after injections at ZT1, ZT3, ZT5, ZT8, ZT10, ZT11, ZT14, ZT18, ZT21, and ZT23. Open circles, DBP mRNA; filled circles, *Rev-erb α* mRNA. For aesthetic reasons, the values obtained at ZT5 and ZT8 are shown at the beginning and the end of the PRC.

Fig. 4. The GR is required for dexamethasone-induced *Per1* expression and phase shifting. (A) Wild-type mice or *GR^{AlfpCre}* mice with a liver-specific disruption of the GR gene were injected at ZT21 with dexamethasone-phosphate (Dex) or solvent as described in the legend to Fig. 3. *Per1* and TBP mRNA accumulations were determined 5 hours after injection in liver, kidney, and heart. The low level of *Per1* transcripts in the liver of the mutant mouse is probably contributed by nonparenchymal liver cells (fibroblasts, Kupffer cells, endothelial cells, etc). (B) Animals were treated as in (A), and DBP and TBP mRNA levels were determined in liver, kidney, and heart at different times.



4A). However, *Per1* expression is only activated in the liver of wild-type mice and remains low in *GR^{AlfpCre}* mice. Hence, a functional GR is necessary for the activation of *Per1* transcription after dexamethasone injection. A similar conclusion can be drawn for dexamethasone-induced phase shifting. DBP mRNA accumulation was delayed by about 3 to 4 hours in liver, kidney, and heart of dexamethasone-injected wild-type mice and in kidney and heart of dexamethasone-injected *GR^{AlfpCre}* mice (Fig. 4B). However, the phase of DBP mRNA accumulation was not affected in the liver of these mutant animals. Thus, the dexamethasone-mediated phase shifting of peripheral oscillators is a tissue-autonomous process.

tained from these data by plotting the amplitudes of positive and negative phase shifts as a function of the circadian time of the dexamethasone injection (Fig. 3D).

The aPRC for liver oscillators shows an important difference from PRCs established for the SCN pacemaker. The PRCs obtained for the central clock consist of three time windows: a dead zone of about 12 hours during which no resetting is observed, and two windows of about 7 to 5 hours during which phase advances and phase delays are observed (26). In contrast, no extended dead zone can be observed in the aPRC of liver, indicating that the phase of

peripheral oscillators can be changed throughout the 24-hour day.

To test whether dexamethasone can act on peripheral oscillators directly by cell-autonomous mechanisms, we examined the effect of dexamethasone on circadian gene expression in mutant mice (*GR^{AlfpCre}*) with a hepatocyte-specific inactivation of the GR gene (27). These mice do not accumulate GRs in hepatocytes and biliary duct cells, which constitute the vast majority of liver cells (27). Five hours after dexamethasone injection (ZT21), *Per1* mRNA accumulation is strongly elevated in kidney and heart of both wild-type and mutant mice (Fig.

The rhythmic secretion of glucocorticoids and their ability to phase shift peripheral clocks makes them valid candidates for signals establishing the link between the SCN pacemaker and peripheral oscillators. Yet, the phases of accumulation cycles for the mRNAs encoding DBP (Fig. 4B) and *Per1*, *Per2*, *Per3*, *Cry1*, and *Rev-erb α* (22) are the same in livers of *GR^{AlfpCre}* mutant and wild-type mice. Therefore, glucocorticoids cannot be the only signals setting the phase of peripheral clocks. That these hormones do, however, play a role in the entrainment of peripheral oscillators is suggested by recent experiments in which peripheral oscillators were uncoupled from the SCN pacemaker by restricted feeding (28).

By exploring glucocorticoid signaling, which does not affect the central circadian pacemaker in the SCN, we have determined that peripheral oscillators can be phase delayed or phase advanced during the entire 24-hour day. This phase-shifting behavior would be expected for slave oscillators that are synchronized by a master pacemaker because they should remain responsive to phase-resetting signals from the SCN at all times.

References and Notes

1. J. C. Dunlap, *Cell* **96**, 271 (1999).
2. S. A. Brown and U. Schibler, *Curr. Opin. Genet. Dev.* **9**, 588 (1999).
3. M. H. Hastings, *Curr. Biol.* **7**, 670 (1997).
4. B. Rusak and I. Zucker, *Physiol. Rev.* **59**, 449 (1979).
5. J. Blau and M. W. Young, *Cell* **99**, 661 (1999).
6. P. L. Lowrey et al., *Science* **288**, 483 (2000).
7. I. F. Emery, J. M. Noveral, C. F. Jamison, K. K. Siwicki, *Proc. Natl. Acad. Sci. U.S.A.* **94**, 4092 (1997).
8. D. Whitmore, N. S. Foulkes, U. Strähle, P. Sassone-Corsi, *Nature Neurosci.* **1**, 701 (1998).
9. A. Balsalobre, F. Damiola, U. Schibler, *Cell* **93**, 929 (1998).
10. S. Yamazaki et al., *Science* **288**, 682 (2000).
11. P. Emery, W. V. So, M. Kaneko, J. C. Hall, M. Rosbash, *Cell* **95**, 669 (1998).
12. R. Stanewsky et al., *Cell* **95**, 681 (1998).
13. M. F. Ceriani et al., *Science* **285**, 553 (1999).
14. D. Whitmore, N. S. Foulkes, P. Sassone-Corsi, *Nature* **404**, 87 (2000).
15. F. Tronche, C. Kellendonk, H. M. Reichardt, G. Schütz, *Curr. Opin. Genet. Dev.* **8**, 532 (1998).
16. P. Rosenfeld, J. A. M. Van Eekelen, S. Levine, E. R. De Kloet, *Dev. Brain Res.* **42**, 119 (1988).
17. ———, *Cell. Mol. Neurobiol.* **13**, 295 (1993).
18. L. Lopez-Molina, F. Conquet, M. Dubois-Dauphin, U. Schibler, *EMBO J.* **16**, 6762 (1997).
19. Rat-1 cells were grown and frozen as described (9). The dexamethasone shock was done as described (9) but with 100 nM dexamethasone (10 mM in ethanol) (Brunschwig AG, Basel, Switzerland). In control petri dishes, 0.001% ethanol in Dulbecco's minimum essential medium (DMEM) with penicillin-streptomycin-glutamine was added.
20. A breeding colony of MORO mice (Swiss mice from RCC Ltd., Füllinsdorf, Switzerland) was established within our temperature-controlled (22° to 24°C) facility in Geneva. GR^{AlpCre} and their respective wild-type control mice were established and housed within a temperature-controlled (20° to 22°C) facility at the Deutsches Krebsforschungszentrum (Heidelberg, Germany). GR^{AlpCre} mice come from a mixed background (129-C57BL/6-FVB/N). All lighting cycles were 12 hours light: 12 hours dark. Male and female mice 8 to 24 weeks of age were used (a single sex was used within the same experiment). Animal care was in accordance with institutional guidelines.
21. Brain cutting, tissue fixation, and in-situ hybridization were performed as described in (18).
22. A. Balsalobre et al., data not shown.
23. Web fig. 1 is available at Science Online at www.sciencemag.org/feature/data/1053506.shl.
24. Injection of 2 mg per kg of body weight (2 mg/kg) of dexamethasone 21-phosphate (400 µg/ml in phosphate-buffered saline (PBS)) (D-1159, Sigma) or solvent (PBS with 0.15% ethanol) was performed intraperitoneally under red light (during the night) or under ambient light (during the day). Dexamethasone-phosphate was used instead of free-dexamethasone (as was used in the in vitro experiments) for solubility reasons. We also confirmed that dexamethasone 21-phosphate produced the same results as dexamethasone in vitro (22).
25. A phase shift is normally defined as a steady-state change in phase that is maintained during a subsequent free-run of the oscillator. The term apparent phase shift response curve (aPRC) was used here because only transient phase shifts could be recorded upon dexamethasone injection. After one cycle, the SCN pacemaker re-established its dominance in the periphery.

26. S. Daan and C. S. Pittendrigh, *J. Comp. Physiol.* **106**, 253 (1976).
27. C. Kellendonk, C. Opherk, K. Anlag, G. Schütz, F. Tronche, *Genesis* **26**, 151 (2000).
28. N. Le Minh, F. Damiola, F. Tronche, C. Kellendonk, G. Schütz, U. Schibler, unpublished data.

29. Supported by the Swiss National Science Foundation, the Louis-Jeantet Foundation for Medicine, and the State of Geneva (U.S.) and by the Deutsche Forschungsgemeinschaft and the European Union (G.S.).

26 June 2000; accepted 11 August 2000

Dendritic Computation of Direction Selectivity by Retinal Ganglion Cells

W. Rowland Taylor,^{1,2*} Shigang He,⁴ William R. Levick,^{2,3} David I. Vaney⁴

Direction-selective ganglion cells (DSGCs) in the retina respond strongly when stimulated by image motion in a preferred direction but are only weakly excited by image motion in the opposite null direction. Such coding represents an early manifestation of complex information processing in the visual system, but the cellular locus and the synaptic mechanisms have yet to be elucidated. We recorded the synaptic activity of DSGCs using strategies to observe the asymmetric inhibitory inputs that underlie the generation of direction selectivity. The critical nonlinear interactions between the excitatory and inhibitory inputs took place postsynaptically within the dendrites of the DSGCs.

In the vertebrate visual system, the encoding of the direction of image motion first occurs in specialized types of retinal ganglion cells, within two or three synapses of the photoreceptor input. These DSGCs have been most extensively studied in the rabbit retina, where two distinct types of DSGCs respond either at the onset and termination of a light stimulus (On-Off DSGCs) or only at the onset of a light stimulus (On DSGCs) (1, 2). The more commonly encountered On-Off DSGCs comprise four physiological subtypes, whose preferred directions are aligned with the horizontal and vertical ocular axes (3).

Extracellular recordings indicate that the key mechanism underlying direction selectivity in DSGCs is spatially asymmetric inhibition, which counteracts excitation for motion in the null direction but not in the preferred direction (2, 4, 5). Pharmacological studies show that γ -aminobutyric acid (GABA) antagonists abolish the direction selectivity of DSGCs, indicating that a GABAergic input from lateral association neurons (amacrine cells) inhibits the excitatory inputs arising from the glutamatergic second-order interneurons (bipolar cells) and from cholinergic amacrine cells (6–8). These studies leave a fundamental question

unanswered: Where do the inhibition and excitation interact? The null-direction inhibition might act presynaptically on the excitatory inputs to the DSGC (Fig. 1, upper panels), in which case the release of transmitter from the excitatory neuron would itself be direction selective. Alternatively, the null-direction inhibition might act postsynaptically on the ganglion cell dendrites (Fig. 1, lower panels) by shunting the excitatory currents through an inhibitory chloride conductance with a reversal potential near the resting potential (shunting inhibition) (7, 9, 10).

Patch-clamp recordings (11) revealed that the On-Off DSGCs generate excitatory postsynaptic potentials (EPSPs) to the leading edge (On response) and trailing edge (Off response) of a light bar moving in any direction through the receptive field, but stimuli moving in the preferred direction produced stronger excitation than stimuli moving in the null direction or in orthogonal directions (Fig. 2A). We measured the On and Off responses to eight directions of motion (12), in terms of both the amplitude of the EPSPs and the number of spikes produced, then plotted the responses in polar coordinates. When the eight individual response vectors are summed, the direction of the resultant vector indicates the preferred direction. This was always similar for the On and Off responses. The length of the resultant vector gives an indication of the strength of the direction selectivity and will tend toward zero for direction-independent responses. EPSPs were elicited by movements in all directions, whereas

¹John Curtin School of Medical Research, ²Centre for Visual Sciences, ³Department of Psychology, Australian National University, Canberra, ACT 2601, Australia. ⁴Vision, Touch and Hearing Research Centre, School of Biomedical Sciences, University of Queensland, Brisbane, QLD 4072, Australia.

*To whom correspondence should be addressed. E-mail: Rowland.Taylor@anu.edu.au